An ab Initio Study of $M^+(CH_3OH)_n$ Clusters (M = K, Rb, Cs). Competition between Interior and Surface Structures

Enrique M. Cabaleiro-Lago*,† and Jesús Rodríguez-Otero‡

Departamento de Química Física, Facultade de Ciencias, Universidade de Santiago de Compostela, Campus de Lugo, Avda Alfonso X El Sabio s/n, 27002 Lugo, Galicia (Spain), and Departamento de Química Física, Facultade de Química, Universidade de Santiago de Compostela, Avda das Ciencias s/n, 15706 Santiago, Galicia (Spain)

Received: March 15, 2002; In Final Form: May 20, 2002

Clusters consisting of a variable number of methanol molecules and K^+, Rb^+, or Cs^+ ions were subjected to ab initio and DFT calculations. Various minima corresponding to interior or surface structures were thus located on the corresponding potential surfaces. In interior structures, methanol molecules interact in a direct manner with the ion but scarcely among themselves; in surface structures, however, the methanol molecules coordinated to the ion also establish hydrogen bonds among them. The $O\cdots M^+$ distance (M = K, Rb, Cs) increases and the strength of the ion−methanol interaction decreases with increasing cluster size. The calculations predict changes in intramolecular geometry that vary very little with cluster size in the interior structures; on the other hand, the presence of hydrogen bonds in the surface clusters results in a significantly lengthened O−H distance, the effect increasing with increase in cluster size. Beyond five methanol molecules, all clusters exhibit hydrogen-bonded structures. In interior clusters consisting of less than 5 molecules, solvent−solvent interactions are of the repulsive type; by contrast, interactions in surface clusters are strongly attractive and increase with increasing cluster or ion size. The incremental binding energy decreases gradually with increasing cluster size but increases as soon as a more stable surface structure is reached by virtue of the additional stabilization introduced by hydrogen bonding. The calculations reproduce the frequency shifts in the O−H stretching mode observed in the Cs^+ clusters; also, they predict a similar spectral behavior for the Rb^+ clusters. The K^+ clusters show smaller shifts that will probably be observed at greater cluster sizes than with the other two ions.

1. Introduction

The solvation of ions by different types of solvents is of interest for a wide variety of applications. Available information about the characteristics of this process can be derived by conducting studies in the gas phase, which facilitate the isolation of individual interactions and hence their characterization.[1−5] In fact, this type of study allows one to explore the nature of the transition between clusters in the gas phase and solvated systems in the liquid phase. In this context, the use of theoretical methods to examine clusters in the gas phase provides a more detailed description of the clusters and information about the mechanisms governing the interaction.

One interesting aspect of the solvation of ions by different solvents is the competition between ion−solvent and solvent−solvent interactions.[1,6,7] In simple ions such as those of the alkaline elements, the electrostatic interaction between the ion and solvent is usually the process governing solvation. Accordingly, the solvent molecules can be expected to surround the ion in order to maximize their interaction with it, forming the so-called interior structures. However, when the solvent can form hydrogen bonds, the interaction between solvent molecules can be more favorable than that with the ion.[1] In this situation, the two phenomena compete with each other and favor the formation of surface structures, where the solvent molecules lie on one side of the ion and interact simultaneously with it and between themselves via hydrogen bonds. This behavior was first observed in mixed clusters of Cs^+ with acetone and methanol,[8] where methanol always occupies the first coordination sphere even though it exhibits a weaker electrostatic interaction than acetone—in fact, the ability of methanol to form hydrogen bonds favors the adoption of such a molecular arrangement.

The significance of this phenomenon is related to the ability of the solvent to establish strong enough hydrogen bonds to overcome the ion−solvent interaction, which is essentially electrostatic in nature. Therefore, the weaker the interaction with the ion (viz., the larger and less charged the ion is), the easier it will be for structures involving hydrogen bonding between the solvent molecules to form. On the other hand, previous studies suggest that the more readily polarized the ion is, the more easily it can form surface structures.[9−12]

One interesting phenomenon involved in the formation of surface structures is the presence of major shifts in the frequencies of the vibration modes associated to hydrogen bonds.[13,14] The formation of a hydrogen bond is known to result in a red shift of up to several hundred reciprocal centimeters in the X−H stretching mode for the donor molecule. Ion−solvent clusters rarely exhibit this type of shift unless the solvent forms hydrogen bonds, either between the molecules in the first coordination sphere or between those in the first and second coordination sphere. Monitoring of these vibration modes

* Corresponding author.
† Departamento de Química Física, Facultade de Ciencias, Universidade de Santiago de Compostela, Campus de Lugo.
‡ Departamento de Química Física, Facultade de Química, Universidade de Santiago de Compostela.

10.1021/jp020713z CCC: $22.00
Published on Web 07/17/2002

provides useful information with a view to determining structural effects in ion−solvent clusters.

Because of the high significance of the properties of water, most studies in this area have focused on aqueous solutions[2−7,9−12,15−22] and only a few have been concerned with the solvation of ions by nonaqueous solvents.[23−29] Like water, methanol can form linear hydrogen bonds that dictate most of their properties in condensed phases. The solvation of various ions by methanol has been experimentally examined using mass spectrometric techniques that allow properties such as enthalpies, entropies, and Gibbs free energy changes to be determined.[23,24,26,30−33] The vibrational spectra for methanol-solvated Cs^+ ion suggest the formation of surface structures in clusters consisting of only 3 methanol molecules.[13] Also, these measurements reveal the presence of different isomers in clusters comprising 3−5 molecules of the alcohol.

In previous work,[29] one of the authors examined clusters consisting of Li^+ or Na^+ ions and up to six methanol molecules. The smallest two alkali ions were then found to form no surface structures with methanol. This resulted in the absence of substantial frequency shifts as the structures concerned involved no hydrogen bonds. However, the cluster consisting of Na^+ and six methanol molecules exhibited a frequency shift that reproduced, at least qualitatively, the experimental shift.[14] Interestingly, it was not a surface structure as the molecules were able to form hydrogen bonds between themselves, keeping a structure where the ion occupied the central position. Also, a major frequency shift was predicted for Li^+ clusters as a result of the hydrogen bonds formed between the molecules in the first and second coordination sphere. However, surface structures can be expected to be most favorable in clusters involving larger ions. In consequence, this paper reports the results obtained from ab initio and DFT calculations on clusters consisting of up to six methanol molecules and the larger alkali ions K^+, Rb^+, and Cs^+.

2. Computational Details

The structure of each cluster was fully optimized using the HF, DFT/B3LYP, and MP2 methods in conjunction with the 6-31+G* basis set for the methanol molecules, and the core effective potential of Hay and Wadt with split-valence basis increased by a Glendening-Feller polarization function for the ions.[12] All calculations were done using the Gaussian 98 software suite.[34] The starting structures were chosen on the basis of chemical intuition and on previously reported configurations for similar clusters with water.[12] Each fully optimized geometry was subjected to vibrational analysis in order to ascertain whether it actually corresponded to a minimum on the potential surface. Taking into account the size of the systems studied, only the HF and DFT/B3LYP frequencies were obtained for the larger clusters; no empirical correction was applied to correct for overestimation. All electrons except those processed using the core effective potential were included in the MP2 calculations. For each optimized structure, the interaction energy and some thermodynamic properties were determined—using ideal-gas thermodynamic functions for the latter.

The interaction energy for an $M^+(CH_3OH)_n$ cluster is the difference between the energy for the cluster in its optimized geometry and those for the fragments that constitute it.[35−37] In mathematical form, this can be expressed as

$$\Delta E_{cl} = E_{cl}(cl) - \sum_{i=1}^{k} E_i(i) \qquad (1)$$

where cl denotes "cluster" and the terms in parentheses the basis set to be used. All interaction energies were corrected from BSSE using the counterpoise method,[35,36,38,39] based on which all energy values are calculated using the basis set for the whole cluster:

$$\Delta E_{cl} = E_{cl}(cl) - \sum_{i=1}^{k} E_i(cl) \qquad (2)$$

For the cluster to form, the resistance of the molecules to adopting their strained geometry in the cluster must be overcome.[37,40] Such a resistance is called "deformation energy" and given by

$$E_{def} = \sum_{i=1}^{n} E^{cl}_{(MeOH)i} - n \cdot E^{isol}_{MeOH} \qquad (3)$$

By adding up this contribution to the interaction energy, one obtains the clustering energy.

To go deeper into the nature of the interaction, particularly as regards the balance between the solvent−solvent and ion−solvent interactions, the total interaction energy was resolved into two contributions corresponding to solvent−solvent and solvent−ion interactions.[6,7] To this end, the solvent−solvent interaction energy was defined as the interaction energy for the cluster formed by the methanol molecules in the cluster geometry:

$$\Delta E_S = E_{(MeOH)n}(cl) - \sum_{i=1}^{n} E_i(cl) \qquad (4)$$

The difference between this quantity and the interaction energy for the cluster will be the ion−solvent interaction energy.

3. Results

This section discusses the results obtained for the clusters consisting of 1−6 methanol molecules and the ions Cs^+, Rb^+, and K^+. The geometries of the clusters are examined first, followed by some energy-related aspects of the solvation. Finally, the frequency shifts predicted by the calculations are analyzed and compared with reported experimental data.

3.1. Cluster Geometries. Figure 1 shows the structures of the minima identified for the clusters consisting of K^+, Rb^+, or Cs^+ and up to four methanol molecules. As can be inferred from the vibrational analysis, where all frequencies were real—no MP2 frequencies were obtained for the clusters consisting of four methanol molecules—, these structures are minima on the corresponding potential surfaces of the clusters with the three calculation methods used. The cluster consisting of a single methanol molecule possesses a structure of C_s symmetry where the cation interacts with the methanol molecule via the oxygen atom, which bears the highest charge density in the methanol molecule. In this configuration, the dipole of the methanol molecule points directly to the cation; this facilitates the charge−dipole interaction, which is the main source of the interaction in this type of system. As can be seen from Table 1, the methanol molecule lies at a distance of 2.63−2.65 Å from the potassium ion. As usual, the incorporation of electron correlation shortens the intermolecular distance (from 2.654 Å at the HF level to 2.630 Å at the MP2 level). This is also the case with the Rb^+ and Cs^+ clusters, where, however, the bond distances are longer (ca. 2.87 Å for Rb^+ and 3.10 Å for Cs^+) as a result of the increased size of the ions. Therefore, the intermolecular

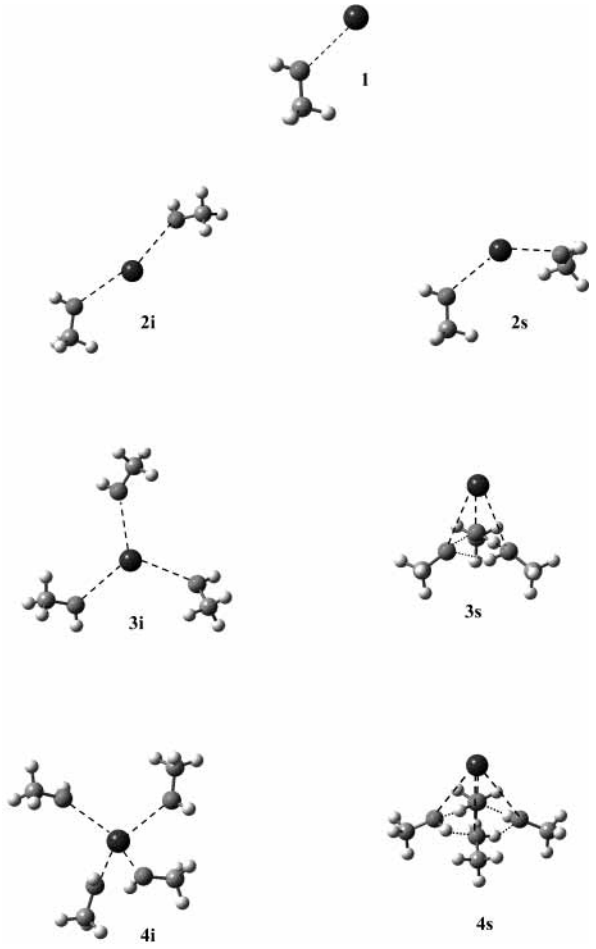

Figure 1. Structure of the minima for the $M^+(CH_3OH)_{1-4}$ clusters.

TABLE 1: Oxygen−Central Ion Intermolecular Distances for the K^+, Rb^+, and Cs^+ Clusters with Methanol

	K^+			Rb^+			Cs^+		
	HF	DFT	MP2	HF	DFT	MP2	HF	DFT	MP2
1	2.654	2.622	2.630	2.891	2.873	2.863	3.127	3.098	3.087
2i	2.691	2.665	2.665	2.926	2.909	2.878	3.172	3.140	3.113
2s	2.691	2.662	2.659	2.926	2.902	2.879	3.163	3.132	3.103
3i	2.720	2.685	2.673	2.954	2.932	2.901	3.196	3.167	3.134
3s	2.720	2.743	2.735	2.996	3.006	2.972	3.256	3.261	3.210
4i	2.751	2.714	2.699	2.983	2.958	2.917	3.224	3.192	3.149
4s	2.810	2.821	2.805	3.066	3.071	3.055	3.325	3.327	3.267
5i	2.867	2.862		3.117	3.124		3.378	3.371	
	2.740	2.699		2.971	2.945		3.215	3.179	
5s	2.884	2.892		3.132	3.141		3.385	3.375	
6i	2.858	2.851		3.101	3.101		3.361	3.351	
6s	3.022	3.711		3.624	3.901		4.069	4.106	
		2.742		2.886	2.997		3.252	3.243	

distance increases by about 0.23 Å from K^+ to Rb^+ and by the same amount from Rb^+ to Cs^+. As stated above, electron correlation shortens intermolecular distances, the effect increasing with increasing ion size (shortening in Cs^+ complex is roughly twice than in K^+ cluster).

The interaction distorts the molecular geometry with respect to the isolated molecule. Table 2 shows the calculated values for the O−H distance in the ion−methanol clusters. The O−H bond distance is lengthened by about 0.003−0.004 Å, the effect being slightly stronger in the K^+ cluster, which is consistent with the stronger interaction to be expected from the increased ion charge/radius ratio.

The incorporation of a second methanol molecule into the ion−solvent cluster can take place in two different ways. In

TABLE 2: Oxygen−Hydrogen Intramolecular Distances for the K^+, Rb^+, and Cs^+ Clusters with Methanol[a]

	K^+			Rb^+			Cs^+		
	HF	DFT	MP2	HF	DFT	MP2	HF	DFT	MP2
1	0.950	0.971	0.975	0.949	0.971	0.976	0.949	0.970	0.975
2i	0.949	0.974	0.975	0.949	0.971	0.974	0.949	0.970	0.974
2s	0.950	0.971	0.971	0.949	0.971	0.975	0.949	0.971	0.975
3i	0.949	0.970	0.974	0.949	0.970	0.974	0.949	0.970	0.975
3s	0.949	0.977	0.981	0.952	0.979	0.982	0.952	0.980	0.982
4i	0.949	0.970	0.974	0.949	0.970	0.974	0.949	0.970	0.973
4s	0.953	0.983	0.986	0.953	0.985	0.988	0.955	0.987	0.989
5i	0.954	0.984		0.955	0.983		0.955	0.987	
	0.949	0.970		0.949	0.971		0.949	0.970	
5s	0.954	0.984		0.954	0.986		0.956	0.987	
6i	0.953	0.981		0.953	0.980		0.953	0.981	
6s	0.954	0.995		1.007	0.994		0.960	0.994	
		0.983		0.989	0.985		0.954	0.986	

(a) Values for the isolated molecule: 0.946 Å; 0.979 and 0.972 Å for HF, DFT/B3LYP and MP2, respectively.

principle, the second molecule would approach with its dipole pointing to the central ion. To maximize this interaction, the two molecules must occupy opposite positions in order to form a virtually linear OMO angle. In this configuration, however, the two molecules would interact repulsively as their dipoles would oppose each other; to minimize this adverse effect, the molecules can adopt an angular configuration where the OMO angle is markedly nonlinear. Structure **2s** can be assumed to be a surface configuration and **2i** an interior configuration. The O···M intermolecular distance always increases upon incorporation of a second molecule. This is the result of the repulsion between methanol molecules, which causes them to depart from each other and increases their distance from the central ion. The greatest lengthening of the intermolecular distance is observed in the K^+ cluster, where the methanol molecules are closer and hence repel each other more strongly; the effect is less marked in the Rb^+ cluster and even less so in the Cs^+ cluster. Structure **2s** behaves similarly but distances are increased to a lesser extent. The intramolecular O−H distances are similar to those in the cluster consisting of a single methanol molecule.

The incorporation of a further methanol molecule to form an $M^+(CH_3OH)_3$ cluster results in two distinct structures (Figure 1). In **3i**, the three methanol molecules surround the ion with their dipoles pointing to it, which favors an ion−dipole interaction. Structure **3s** is a typical surface configuration where the methanol molecules interact with the ion and, simultaneously, with one another, to form hydrogen bonds. In this structure, the interaction between solvent molecules can partly overcome the ion−dipole interaction and result in a less favorable arrangement for this type of interaction. Both **3i** and **3s** correspond to minima on the potential surface for all the ions and computational methods considered except the K^+ cluster with HF. This is a result of the HF method overestimating the molecular dipole (thereby favoring the ion−dipole interaction in the interior structure) and underestimating the interaction between solvent molecules. Because it is the smallest and least polarizable of the three ions —and hence that with the lowest tendency to forming surface structures—, K^+ exhibits no **3s** structure with the HF method as the interaction between the methanol molecules is not strong enough to distort the interior structure and yield the corresponding surface structure.

Obviously, these two structures will behave differently, particularly as regards the characteristics of the methanol molecules in the cluster. Structure **3i** exhibits an additional increase in O···M distance when the third molecule is incorporated; this suggests that the ion−solvent interaction is

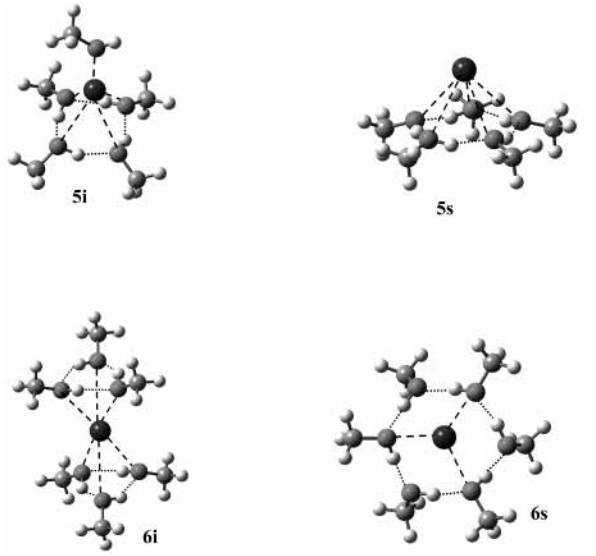

Figure 2. Structure of the minima for the $M^+(CH_3OH)_{5,6}$ clusters.

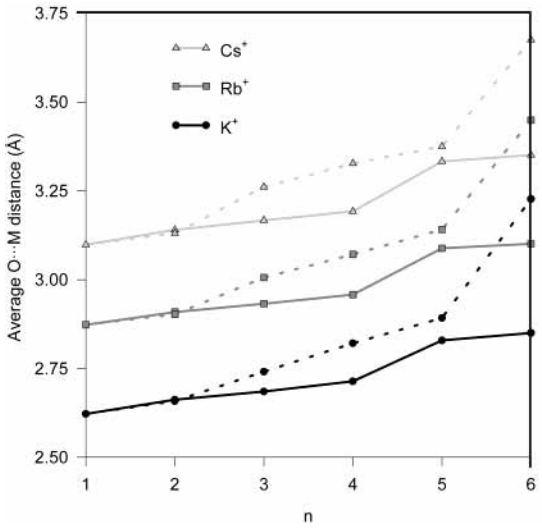

Figure 3. Variation of the O−X distance with cluster size as calculated using the DFT/B3LYP method. (—) Interior structures. (- - -) Surface structures.

weakened by repulsions between methanol molecules in this structure. In structure **3s**, the O···M distance is longer than in the interior structure (0.06, 0.07, and 0.09 Å longer in the K^+, Rb^+, and Cs^+ cluster, respectively). The differential behavior of structures **3s** and **3i** also reflects in the O−H distance, which exhibits molecular distortion by effect of the interaction. Thus, in **3i**, the O−H distance is similar to that observed in smaller clusters or even slightly shorter since the ion−methanol interaction weakens as further molecules are added. On the other hand, in **3s**, the O−H distance is substantially longer (0.07−0.10 Å) than in the interior structure. This increase is not directly related to the interaction of the molecules with the ion, but rather arises from the hydrogen-bonding interaction between the methanol molecules. The strongest distortion is observed with the largest ion, which allows the methanol molecules to interact in the most favorable manner.

In the clusters consisting of four methanol molecules, the situation is similar to that in the $M^+(CH_3OH)_3$ cluster. Again, two minima are observed on the potential surface for all the ion−solvent clusters studied. In structure **4i**, the methanol molecules lie with their oxygen atoms occupying the vertexes of a tetrahedron; in the other minimum, **4s**, they interact with one another via hydrogen bonds. In **4i**, intermolecular distances are lengthened by a further 0.02−0.03 Å with respect to **3i**. In **4s**, O···X distances are 0.07−0.08 Å longer than in **3s** with the three ions studied. Also, structure **4i** exhibits no changes in O−H distances, whereas **4s** experiences and additional lengthening by 0.006 Å; this shows that the interaction between methanol molecules is even more favorable than in the trimer.

The study was extended to clusters of five and six methanol molecules, but using the HF and DFT/B3LYP methods only for computational economy. On the basis of the structures identified in the smaller clusters, we focused on the four minima shown in Figure 2. For the cluster consisting of five methanol molecules, we considered a structure where a cyclic pentamer interacted with the ion (**5s**) and another where the methanol molecules occupied the vertexes of a square-base pyramid (**5i**). Attempts at identifying a trigonal bipyramid structure were unsuccessful. Structures **5i** and **5s** correspond to an interior and surface configuration, respectively. Unlike smaller clusters, both structures can form hydrogen bonds. In **5i**, the methanol molecules are not equivalent as four interact with one another to form a tetramer whereas the fifth interacts with the ion on the opposite side. The O···M distances in the molecules forming the tetramer are longer than in any of the smaller clusters; on the other hand, the remaining molecule lies closer to the ion —at a distance similar to those observed in the $M^+(CH_3OH)_3$ cluster. Also, the O−H distances also discriminate between the methanol molecules. Thus, four of the distances are very similar to that in the surface cluster consisting of four molecules, whereas the other is similar to that found in the interior clusters. In **5s**, the interaction involves the ion and five methanol molecules connected by hydrogen bonds. Intermolecular distances are longer than in any of the previous clusters, and so is the case with intramolecular O−H distances, which are slightly longer than in **4s**.

Finally, we examined two structures for clusters consisting of six methanol molecules. In one, **6i**, two trimers connected by hydrogen bonds lay on both sides of the cation; in the other, the six methanol molecules were linked to one another via hydrogen bonds and formed a hexamer. Intermolecular distances in **6i** are no longer, but rather shorter than those in **5i**, and so is the case with O−H distances. Structure **6s** exhibits two distinct types of molecules; three interact more closely with the cation and the other three interact with the previous ones via hydrogen bonds forming a chair configuration. Only K^+, with the HF method, departed from this behavior and exhibits a cyclic hexamer of C_6 symmetry bonded to the cation. The group encompassing the three molecules that interact with the cation exhibits relatively short O···X distances that are similar to those in **3s**. On the other hand, the other three molecules are much more distant (0.8−1.0 Å more). This differential behavior also reflects in the O−H distances: the molecules closer to the cation, which interact more strongly with it, possess longer O−H distances than those in the clusters of smaller size; on the other hand, the other three molecules exhibit shorter (0.01 Å) distances that are similar to those in **4s**.

Figures 3 and 4 show the above-described trends in the O···X and O−H distances for the different clusters studied. As can be seen from Figure 3, surface and interior structures behave markedly differently; the former invariably exhibit longer O···X distances. As cluster size increases, distances increase to a similar extent in both types of structure, the main difference arising in the cluster consisting of six methanol molecules. Thus, while the distance varies only slightly in the interior structure, it changes markedly in the surface structure. This behavior is associated with the fact that the graph shows average distances,

TABLE 3: Interaction Energies (kcal/mol) for the $M^+(CH_3OH)_n$ Clusters (numbers in parentheses are deformation energies)

	K^+			Rb^+			Cs^+		
	HF	DFT	MP2	HF	DFT	MP2	HF	DFT	MP2
1	−19.27 (0.31)	−19.46 (0.28)	−20.25 (0.26)	−16.20 (0.24)	−16.13 (0.22)	−17.40 (0.21)	−13.84 (0.20)	−13.85 (0.18)	−13.96 (0.18)
2i	−36.20 (0.50)	−36.19 (0.45)	−38.19 (0.43)	−30.57 (0.40)	−30.24 (0.35)	−32.75 (0.31)	−26.02 (0.32)	−26.05 (0.29)	−28.81 (0.29)
2s	−36.19 (0.50)	−36.55 (0.45)	−37.86 (0.38)	−30.57 (0.40)	−30.45 (0.35)	−32.75 (0.31)	−26.14 (0.32)	−26.18 (0.29)	−28.73 (0.28)
3i	−50.87 (0.58)	−51.23 (0.51)	−53.43 (0.45)	−43.23 (0.48)	−42.98 (0.42)	−46.55 (0.38)	−37.06 (0.40)	−36.98 (0.39)	−41.07 (0.35)
3s	−50.87 (0.58)	−49.72 (0.80)	−53.37 (0.78)	−40.99 (0.50)	−43.49 (0.80)	−47.98 (0.77)	−36.15 (0.46)	−39.19 (0.80)	−43.61 (0.75)
4i	−63.03 (0.58)	−63.45 (0.51)	−67.32 (0.48)	−54.03 (0.50)	−53.73 (0.44)	−59.10 (0.41)	−47.40 (0.45)	−46.39 (0.38)	−51.97 (0.36)
4s	−59.72 (0.73)	−64.42 (1.36)	−68.29 (1.29)	−52.95 (0.70)	−58.26 (1.38)	−63.00 (1.31)	−47.73 (0.67)	−53.51 (1.42)	−58.42 (1.32)
5i	−72.75 (0.84)	−78.14 (0.95)		−64.53 (0.75)	−70.03 (0.86)		−57.84 (0.65)	−63.97 (0.82)	
5s	−69.17 (0.83)	−75.43 (1.61)		−62.55 (0.82)	−69.12 (1.69)		−57.16 (0.79)	−64.85 (1.72)	
6i	−82.24 (0.82)	−88.40 (1.39)		−73.20 (0.78)	−79.27 (1.46)		−65.59 (0.74)	−72.53 (1.46)	
6s	−74.65 (0.93)	−88.59 (1.61)		−65.10 (0.78)	−81.21 (2.57)		−65.28 (0.99)	−75.68 (2.34)	

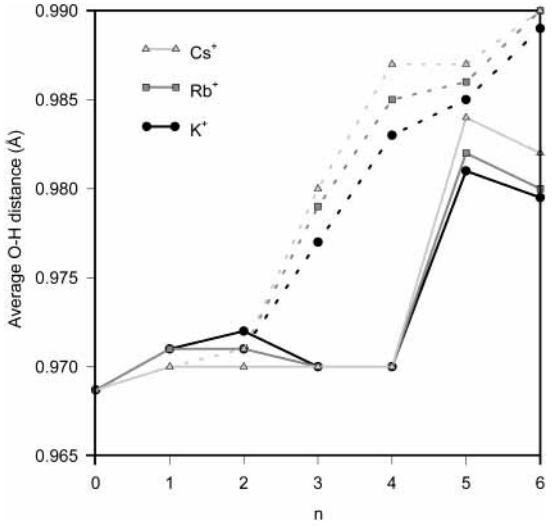

Figure 4. Variation of the O−H distance with cluster size as calculated using the DFT/B3LYP method. (—) Interior structures. (- - -) Surface structures.

and structure **6s** possesses a very long and a relatively short distance, which results in a large average value relative to the other clusters. This also results in the anomalously large distance observed in structure **5i**. Figure 4 shows the variation of the average O−H distance with cluster size; as can be seen, surface and interior structures exhibit a distinct behavior. After an initial increase, the interior structures experience a slight shortening of the O−H distance up to $n = 4$, followed by a marked increase at $n = 5$ and a subsequent decrease at $n = 6$. This behavior is related to the presence of hydrogen bonds in the clusters of five and six methanol molecules, which causes a substantial lengthening of the O−H distance. The cluster of $n = 5$ encompasses a tetramer of methanol molecules connected via hydrogen bonds, so the O−H distances are similar to those for the surface structure of $n = 4$ (though slightly shorter). At $n = 6$, two trimers exist the O−H distances in which are intermediate between those in the surface structures of $n = 3$ and $n = 4$. The surface structures behave rather differently. In fact, the O−H distance increases gradually with increasing cluster size, which suggests that the hydrogen-bonding interaction becomes stronger as further methanol molecules are incorporated into surface structures.

3.2. Energies. The interaction energies for the optimized cluster structures shown in Figures 1 and 2 were obtained using the three HF, DFT/B3LYP and MP2 methods as described in Section 2. The energies for the clusters consisting of five or six methanol molecules, however, were calculated using the former two only. The results are shown in Table 3. As can be seen, the three computational methods provided fairly similar results, so electron correlation appears to be insubstantial in this type of cluster, where the interaction is essentially electrostatic in nature, though larger differences are observed in surface structures, where solvent−solvent interactions are more relevant. The clusters consisting of a single methanol molecule and K^+, Rb^+, and Cs^+ exhibit an interaction energy of −20, −17, and −14 kcal/mol, respectively. The energy decreases by about 3 kcal/mol as the radius of the ion increases because the methanol molecule must lie increasingly distant from it—which decreases the ion−dipole interaction. The three computational methods used provide similar values, and only MP2 gives slightly more attractive energies.

As stated above, the cluster consisting of two methanol molecules exhibits two possible structures with a very similar interaction energy (the difference is only a few tenths of a kcal/mol). The incorporation of the second methanol molecule causes an energy change about 2 kcal smaller than that involved in the formation of the single-molecule cluster. This is a result of the interaction weakening as successive molecules are incorporated by effect of the above-described increase in molecular distance. The decrease affects all interior structures. To obtain more detailed information about the interaction, the solvent−solvent interaction, as defined by eq 4, was calculated for each cluster, the results being shown in Table 4. As can be seen, the interaction in the clusters of two molecules is slightly repulsive, which has a destabilizing effect by virtue of the dipoles facing each other. Repulsion decreases with increasing ion size (i.e., with increasing distance between the molecules).

As with the geometries, the cluster consisting of three methanol molecules exhibits a more distinct behavior. Thus, structure **3i** is predicted to be the most stable in the K^+ clusters with the three methods, and also in the Rb^+ cluster with HF. On the other hand, the incorporation of electron correlation favors structure **3s** in the Rb^+ and Cs^+ clusters. This is a result of the greater ease with which the larger cations can form surface structures and is apparent from Table 4: structure **3i** exhibits a repulsive interaction between the solvent molecules (ca. 2 kcal/mol), whereas structure **3s** exhibits an attractive interaction that increases with increasing ion size. Thus, the interaction energy per hydrogen bond changes from ca. −3 kcal/mol in the K^+ cluster to −4 kcal/mol in the Cs^+ cluster. The HF values are much lower than those provided by the other two methods and amount to barely one-half of the DFT/B3LYP values.

The situation is similar in the cluster of four molecules, for which only the HF method points to the interior structure as the most stable in the K^+ and Rb^+ clusters. The incorporation of the fourth molecule allows the solvent molecules to interact more readily with one another in the surface structure and increases repulsion in the interior structure. As a result, structure **4s** is the most stable in most instances. In this case, the interaction energy per hydrogen bond for the surface structure

TABLE 4: Contribution of the Interaction between Solvent Molecules to the Overall Interaction Energy (kcal/mol)

	K^+			Rb^+			Cs^+		
	HF	DFT	MP2	HF	DFT	MP2	HF	DFT	MP2
2i	0.86	0.77	0.81	0.71	0.53	0.32	0.48	0.48	0.71
2s	0.85	0.84	0.55	0.70	0.70	0.32	0.61	0.56	0.14
3i	2.91	2.84	1.65	2.28	2.20	2.65	1.82	1.75	1.87
3s	2.91	−8.72	−9.36	−5.65	−11.07	−11.01	−7.43	−12.36	−12.09
4i	6.25	6.06	5.46	4.91	4.75	4.64	4.26	3.85	3.90
4s	−9.74	−18.95	−18.66	−13.26	−21.32	−21.09	−15.24	−22.99	−22.14
5i	−9.95	−18.32		−13.09	−20.99		−15.04	−22.55	
5s	−14.32	−25.32		−18.52	−28.55		−21.02	−30.15	
6i	−9.38	−19.39		−13.30	−22.78		−16.04	−25.01	
6s	−19.80	−38.09		−23.63	−39.56		−28.72	−40.49	

is −4.7 kcal/mol for the K^+ cluster and −5.7 kcal/mol for the Cs^+ cluster. These values are much greater than those for the clusters of three molecules, possibly as a result of cooperativeness in the interaction, which is known to increase hydrogen-bonding interactions in methanol clusters;[41] however, it may also be the result of the molecules being able to adopt a more favorable structure to interact with one another in the four-molecule cluster.

The situation is different in the clusters of five methanol molecules as all structures can form hydrogen bonds. As a result, the differences in interaction energy between both types of structure are not so large as in the smaller clusters and the interior structure is more stable in most instances. In fact, the hydrogen-bonding interaction energy in the interior structure is −3.8 to −4.5 kcal/mol and thus lower than in the four-molecule cluster. By contrast, the energy in the surface structure exhibits a further increase, reaching −5.1 kcal/mol for the K^+ cluster and −6.0 kcal/mol for the Cs^+ cluster, that is related to cooperativeness or a more suitable geometric arrangement in the methanol molecules.

Both types of structure form hydrogen bonds in the six-molecule clusters; however, the surface structure is invariably the most stable. The hydrogen-bonding interaction energy is −3 to −4 kcal/mol for the interior structure and thus lower than that for the cluster of four molecules. In structure **6s**, the hydrogen-bonding interaction energy is −6.4 kcal/mol for the K^+ cluster and −6.75 kcal/mol for the Cs^+ cluster (i.e., higher than those for the smaller clusters). This is so even though three of the molecules do not interact directly with the ion. However, the three molecules that do interact with the cation are strongly perturbed, and establish especially intense hydrogen-bonding interactions with the other three molecules in the cluster. This behavior had previously been observed in Li^+ clusters,[29] where a hydrogen bond between the first and second coordination spheres was found to be particularly strong.

Table 3 also shows deformation energies for each cluster as calculated by using eq 3. Though interaction in this kind of cluster is quite strong, deformation energies constitute a small percentage (1−3%) of the total interaction energy. However, a distinct behavior is observed for interior and surface structures. In interior structures deformation energies are small, with values decreasing as the size of the central ion increases, thus reflecting the decrease on ion−solvent interaction. However, in surface structures (or interior ones with $n > 4$) deformation energies are larger as a consequence of hydrogen bonding among methanol molecules, usually increasing with the size of the ion. This effect can be ascribed to a more favorable arrangement of methanol molecules in clusters of larger ions, which permits a stronger solvent−solvent interaction, resulting in larger deformation energies. Also, a cooperative enhancement of the hydrogen bond interaction could be partly responsible of the large deformation energies observed in surface structures.

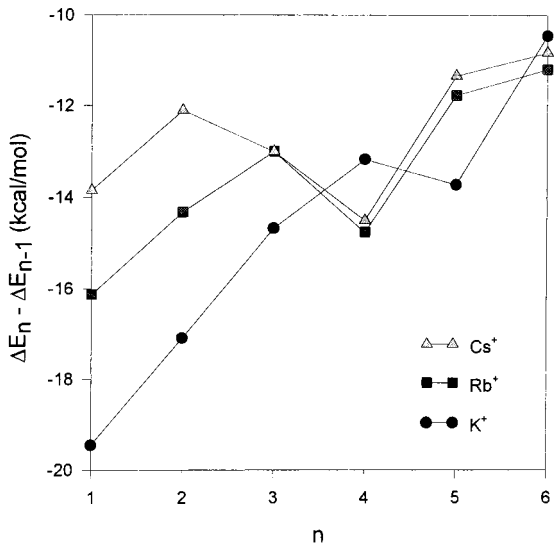

Figure 5. Variation of the incremental binding energy ($\Delta E_n - \Delta E_{n-1}$) with cluster size as calculated with the DFT/B3LYP method.

Figure 5 shows the incremental binding energy, i.e., $\Delta E_n - \Delta E_{n-1}$, as calculated for the most stable structure in each cluster using the DFT/B3LYP method. As can be seen, the energy for the K^+ clusters decreases with increasing cluster size through a decreased ion−molecule interaction. This trend holds virtually linearly up to $n = 4$; however, the incorporation of a further molecule introduces additional stability, so the incremental binding energy is more exothermic. This behavior is clearly related to the presence of hydrogen bonds in the structure. Up to $n = 4$, the molecules form no hydrogen bonds in the most stable K^+ clusters, so the decrease in binding energy results from repulsions between the methanol molecules. The five-molecule cluster, however, exhibits hydrogen bonds that introduce additional stability with respect to the structures that form none. The incremental binding energy again decreases in the cluster of $n = 6$ as it represents the difference between two structures that form hydrogen bonds. The Rb^+ clusters exhibit a similar trend, which, however, changes at $n = 4$ (where the surface structure is more stable than the interior structure). Again, the change is due to the presence of hydrogen bonds. In the Cs^+ cluster, the incremental binding energy starts to be more exothermic at $n = 3$, where the surface structure is more stable than the interior structure.

To derive more detailed information about the hydrogen-bonding interaction in these clusters, we examined the variation of the O···H distance and hydrogen-bonding energy in the surface structures. As can be seen from Figure 6, the strength of the hydrogen bonds doubled with increase in cluster size from $n = 3$ to $n = 6$, the largest variations being observed from $n = 3$ to $n = 4$ and from $n = 5$ to $n = 6$. Also, the O···H distance

TABLE 5: Selected Thermodynamic Properties (kcal/mol) for the $M^+(CH_3OH)_n$ Clusters at 298 K As Calculated Using the DFT/B3LYP Method

	K^+			Rb^+			Cs^+		
	D_0	ΔH	ΔG	D_0	ΔH	ΔG	D_0	ΔH	ΔG
1	−18.49	−18.79	−12.59	−15.27	−15.50	−9.52	−13.06	−13.26	−7.45
2i	−34.20	−34.00	−20.14	−28.56	−28.73	−14.64	−24.51	−24.61	−10.61
2s	−34.61	−34.37	−21.77	−28.74	−28.36	−16.65	−24.58	−24.78	−11.93
3i	−48.40	−47.59	−27.75	−40.50	−39.46	−21.28	−34.87	−35.92	−10.52
3s	−45.20	−45.48	−19.24	−38.98	−39.23	−13.01	−34.69	−34.92	−8.20
4i	−59.85	−58.42	−31.51	−50.53	−48.84	−22.96	−43.47	−41.60	−17.13
4s	−57.91	−58.28	−21.43	−51.82	−52.16	−15.32	−47.20	−47.45	−11.24
5i	−70.76	−70.54	−27.51	−62.90	−63.10	−18.53	−56.94	−57.65	−11.06
5s	−67.55	−67.66	−21.55	−61.20	−61.29	−14.71	−56.96	−57.06	−10.40
6i	−79.29	−79.02	−25.11	−70.33	−70.49	−15.32	−63.57	−63.12	−10.90
6s	−78.91	−79.00	−23.71	−71.70	−72.27	−16.78	−66.24	−66.19	−11.40

TABLE 6: Principal Frequency Shifts (cm^{-1}) in the O−H Stretching Mode in the $M^+(CH_3OH)_n$ Clusters (signal intensities in km/mol are shown in italics). DFT/B3LYP Results.[a]

	interior structures							surface structures					
	K^+		Rb^+		Cs^+			K^+		Rb^+		Cs^+	
1	−18	*65*	−17	*57*	−18	*52*	**1**						
2i	−16	*77*	−15	*61*	−15	*25*	**2s**	−17	*65*	−16	*74*	−16	*73*
	−16	*42*	−15	*46*	−15	*72*		−16	*55*	−16	*34*	−16	*25*
3i	−15	*54*	−15	*49*	−12	*45*	**3s**	−132	*13*	−180	*6*	−215	*4*
	−14	*55*	−14	*50*	−12	*46*		−112	*314*	−150	*439*	−178	*517*
	−14	*53*	−14	*49*	−11	*45*		−111	*310*	−149	*435*	−176	*516*
4i	−12	*59*	−13	*49*	−13	*53*	**4s**	−267	*13*	−313	*7*	−354	*4*
	−12	*42*	−13	*41*	−13	*33*		−225	*1011*	−262	*1195*	−293	*1346*
	−11	*44*	−12	*45*	−13	*31*		−225	*1011*	−262	*1196*	−293	*1346*
	−11	*47*	−12	*44*	−13	*49*		−205	*0*	−238	*0*	−266	*0*
5i	−292	*10*	−337	*8*	−367	*4*	**5s**	−305	*18*	−355	*10*	−382	*7*
	−245	*1101*	−282	*1297*	−305	*1401*		−262	*1581*	−302	*1863*	−325	*1972*
	−245	*1099*	−277	*1284*	−301	*1388*		−262	*1582*	−302	*1863*	−325	*1972*
	−223	*1*	−253	*9*	−274	*4*		−230	*0*	−265	*0*	−285	*0*
	−15	*52*	−19	*48*	−14	*44*		−230	*0*	−265	*0*	−285	*0*
6i	−183	*12*	−212	*7*	−235	*12*	**6s**	−474	*435*	−476	*308*	−479	*230*
	−183	*0*	−212	*1*	−235	*6*		−446	*1442*	−443	*1580*	−441	*1672*
	−153	*0*	−176	*1*	−194	*0*		−444	*1416*	−440	*1570*	−437	*1698*
	−153	*0*	−174	*1029*	−193	*1141*		−248	*637*	−277	*667*	−298	*658*
	−151	*877*	−174	*4*	−189	*1*		−247	*637*	−275	*668*	−296	*665*
	−151	*872*	−172	*1026*	−188	*1122*		−247	*636*	−274	*658*	−292	*662*

[a] Values for the isolated molecule: 3764 cm^{-1}; *24* km/mol.

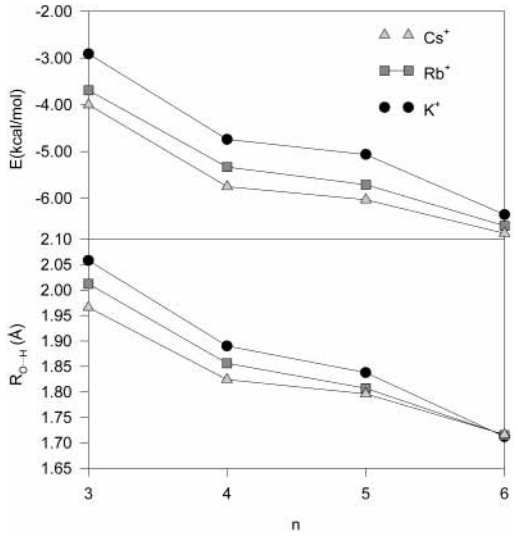

Figure 6. Variation of the energy per hydrogen bond and O···H distance in the surface structures obtained with the DFT/B3LYP method.

decreased gradually with increase in cluster size. The three ions exhibit a similar behavior that appears to converge at $n = 6$.

Table 5 shows the values of selected thermodynamic parameters for the clusters as calculated using the DFT/B3LYP method. An experimental enthalpy of association for the $K^+(CH_3OH)$ cluster of −21.9 kcal/mol has been reported in the literature that is −3 kcal/mol lower than our calculated value.[33] However, this experimental datum has been questioned by some authors,[22] who have estimated it to be ca. −20 kcal/mol and hence closer to our calculations. In fact, the MP2 method provided a value of −19 kcal/mol and using a larger basis set [6-311++g(2d,2p)] yielded a similar value. We can thus assume our estimates to be reasonably accurate. As can be seen from Table 5, the incorporation of the zero-point correction or thermal effects results in no appreciable change in cluster stability. On the other hand, the incorporation of entropic effects causes highly significant changes, particularly in the clusters of $n = 3$ and $n = 4$, where the interior structure is much more favored than the surface structure.

3.3. Frequency Shifts. The interaction in clusters is known to cause shifts in the frequency of some vibrational normal modes strongly involved in it. Thus, shifts in the O−H stretching frequency were used by Weiheimer et al.[13] to study clusters of methanol with Cs^+ ion. They concluded that clusters with only three molecules exhibited significant red shifts (about −250 cm^{-1}), as well as an additional band close to the original frequency. Larger clusters also exhibited frequency shifts as the band at the original frequency gradually weakened and eventually disappeared in the six-molecule cluster.

Table 6 shows the O−H stretching frequency shifts for the different structures studied in this work. The formation of a cluster between a Cs^+ ion and a single methanol molecule shifts the stretching frequency by about -20 cm^{-1}. The incorporation of a second methanol molecule results in a similar, but smaller shift. If interior structures are considered in isolation, then shifts are all of the previous order of magnitude but decrease with increasing cluster size. The clusters of $n > 4$ exhibit strong shifts associated to the hydrogen bonds also present in the interior structures. The situation is completely different in the surface structures. Thus, the cluster of $n = 3$ exhibits a frequency shift of -178 cm^{-1} and a strong increase in the intensity of the band (by up to 20 times). The presence of two bands in the experimental spectrum allows one to assume the occurrence of both the surface and, particularly, the interior structure. Our results are consistent with this trend: while the surface structure is the more stable at 298 K, the entropic factor favors the interior structure. The clusters of $n = 4$ exhibit greater shifts (up to -293 cm^{-1}) that are consistent with their experimental counterparts. Shifts are somewhat larger (-325 cm^{-1}) in the five-molecule clusters, where the original band is virtually absent judging by the calculations. The spectra for clusters of $n = 4,5$ show one additional peak that is not predicted by the calculations. The discrepancies should be ascribed to other isomers present in the sample. As indicated by Weiheimer and Lisy[13] there seem to be at least four different environments for methanol in these clusters, corresponding to structural arrangements that could differ from those considered in this work. Finally, the six-molecule cluster exhibits a single band, shifted by about -300 to -500 cm^{-1}, which is consistent with the experimental results, though discrepancies are larger. In any case, these values should be taken cautiously since the approximations involved in calculating harmonic frequencies can introduce significant errors, though we believe the principal conclusions are valuable.

Based on the data of Table 6, Rb^+ clusters with methanol should behave similarly, with smaller shifts (about 30 cm^{-1} in most cases). The red-shifted band in the cluster of $n = 3$ should be weaker as the structure is less favorable in the Rb^+ cluster. The calculations for the K^+ clusters predict even smaller shifts (about 40 cm^{-1} smaller than for the Rb^+ clusters); also, the band associated to **3s** should not appear in the K^+ clusters as this structure is less favorable than in the clusters of the other two ions. In all other respects, the K^+ clusters should behave similarly to the others.

4. Conclusions

In this work, ab initio and DFT calculations on clusters consisting of the cations K^+, Rb^+, and Cs^+ and up to six methanol molecules were performed. A wide variety of structures were characterized that were found to correspond to minima on the potential surface for each cluster. The results were similar with the three computational methods used; however, the HF method tended to underestimate the significance of interactions between the solvent molecules, and hence to favor the interior structures.

The analysis of cluster geometries allowed clear-cut differences between interior and surface structures to be established. In the surface structures, the distances between the oxygen atoms and the central ion exceeded those in the interior structures of identical size. On the other hand, the O−H distances in the methanol molecules underwent substantial lengthening with respect to the isolated molecule in the surface structures of the clusters with $n < 5$ by effect of the hydrogen-bonding interaction. In larger clusters, all structures were found to exhibit hydrogen bonds and hence lengthened O−H distances.

Incremental binding energies where found to be monotonically less exothermic with increase in cluster size in interior structures up to $n = 4$. However, a significant deviation was observed for interior structures with $n > 5$ or when a surface structure was more stable than the corresponding interior one, as the hydrogen bonds present in the structure introduced additional stability not possible in smaller clusters. This change in the trend observed in smaller clusters signals the cluster size where hydrogen bonds are present in the most stable complex. The energy of interaction between methanol molecules is of the repulsive type in the interior structures but strongly stabilizing in the surface structures, being more favorable as the cluster size increases. This phenomenon may be related to cooperativeness in the hydrogen bonds or to the prevailing structural arrangement favoring the interaction between the solvent molecules as the cluster growths.

The analysis of the frequency shifts in the O−H stretching mode reveals the presence of large shifts resulting from the presence of hydrogen bonds. The calculations reproduce the experimental results for the Cs^+ clusters; however, the analysis of larger clusters is rendered more complicated by the possibility of several different structures exhibiting different frequency shifts coexisting in them. Based on the results obtained for the other clusters, the Rb^+ clusters can be assumed to behave very similarly in spectral terms, though exhibiting smaller shifts; on the other hand, the K^+ clusters will exhibit even smaller frequency shifts that will probably be observed at greater cluster sizes than with the other two ions.

References and Notes

(1) Stace, A. J. *Phys. Chem. Chem. Phys.* **2001**, *3*, 1935.
(2) Dzidic, I.; Kebarle, P. *J. Phys. Chem.* **1970**, *74*, 1466.
(3) Keesee, R. G.; Castleman, A. W., Jr. *J. Phys. Chem. Ref. Data* **1986**, *15*, 1011.
(4) Searles, S. K.; Kebarle, P. *Can. J. Chem.* **1969**, *47*, 2619.
(5) Steel, E. A.; Merz, K. M. J.; Selinger, A.; Castleman, A. W., Jr. *J. Phys. Chem.* **1995**, *99*, 7829.
(6) Hashimoto, K.; Morokuma, K. *J. Am. Chem. Soc.* **1994**, *116*, 11436.
(7) Hashimoto, K.; He, S.; Morokuma, K. *Chem. Phys. Lett.* **1993**, *206*, 297.
(8) Selegue, T. J.; Cabarcos, O. M.; Lisy, J. M. *J. Chem. Phys.* **1994**, *100*, 4790−4796.
(9) Kaupp, M.; Schleyer, P. v. R. *J. Phys. Chem.* **1992**, *96*, 7316.
(10) Kaupp, M.; Schleyer, P. v. R.; Stoll, H.; Preuss, H. *J. Chem. Phys.* **1991**, *94*, 1360.
(11) Kaupp, M.; Schleyer, P. v. R. *J. Am. Chem. Soc.* **1992**, *114*, 491.
(12) Glendening, E. D.; Feller, D. *J. Phys. Chem.* **1995**, *99*, 3060.
(13) Weinheimer, C. J.; Lisy, J. M. *Int. J. Mass Spectrom. Ion Processes* **1996**, *159*, 197.
(14) Weinheimer, C. J.; Lisy, J. M. *J. Phys. Chem.* **1996**, *100*, 15305.
(15) Bauschlicher, C. W. J.; Langhoff, S. R.; Partridge, H.; Rice, J.; Komornicki, A. *J. Chem. Phys.* **1991**, *95*, 5142.
(16) Combariza, J. E.; Kestner, N. R. *J. Chem. Phys.* **1995**, *99*, 2717.
(17) Feller, D.; Glendening, E. D.; Kendall, R. A.; Peterson, K. A. *J. Chem. Phys.* **1994**, *100*, 4981.
(18) Feller, D.; Glendening, E. D.; Woon, D. E.; W, F. M. *J. Chem. Phys.* **1995**, *103*, 3526.
(19) Mhin, B. J.; Kin, J.; Kim, K. S. *Chem. Phys. Lett.* **1993**, *216*, 305.
(20) Xantheas, S. S.; Dunning, T. H. J. *J. Phys. Chem.* **1992**, *96*, 13489.
(21) Xantheas, S. S.; Dunning, T. H. J. *J. Phys. Chem.* **1994**, *98*, 13489.
(22) Nielsen, S. B.; Masella, M.; Kebarle, P. *J. Phys. Chem. A* **1999**, *103*, 9891−9898.
(23) Guo, B. C.; Conklin, B. J.; Castleman, A. W., Jr. *J. Am. Chem. Soc.* **1989**, *111*,
(24) Guo, B. C.; Castleman, A. W., Jr. *Atoms, Molecules Clusters* **1991**, *19*, 397.
(25) Davidson, W. R.; Kebarle, P. *J. Am. Chem. Soc.* **1976**, *98*, 6125.
(26) Rodgers, M. T.; Armentrout, P. B. *J. Phys. Chem. A* **1997**, *101*, 2614.
(27) Cabaleiro-Lago, E. M.; Ríos, M. A. *Chem. Phys.* **2000**, *254*, 11.

(28) Islam, M. S.; Pethrick, R. A.; Pugh, D. *J. Phys. Chem. A* **1998**, *102*, 1089.

(29) García-Muruais, A.; Cabaleiro-Lago, E. M.; Hermida-Ramón, J. M.; Rios, M. A. *Chem. Phys.* **2000**, *254*, 109.

(30) Hiraoka, K.; Yamabe, S. *Int. J. Mass Spectrom. Ion Processes* **1991**, *109*, 133.

(31) Kebarle, P.; Caldwell, G.; Magnera, T.; Sunner, J. *Pure Appl. Chem.* **1985**, *57*, 339.

(32) Woodward, C. A.; Dobson, M. P.; Stace, A. J. *J. Phys. Chem. A* **1997**, *101* (12), 2279.

(33) Evans, D. H.; Keese, R. G.; Castleman, A. W., Jr. *J. Phys. Chem.* **1991**, *95*, 3558.

(34) Frisch, M. J.; Trucks, G. W.; Schlegel, H. B.; Scuseria, G. E.; Robb, M. A.; Cheeseman, J. R.; Zakrzewski, V. G.; Montgomery, J. A.; Stratmann, R. E.; Burant, J. C.; Dapprich, S.; Millam, J. M.; Daniels, A. D.; Kudin, K. N.; Strain, M. C.; Farkas, O.; Tomasi, J.; Barone, V.; Cossi, M.; Cammi, R.; Mennucci, B.; Pomelli, C.; Adamo, C.; Clifford, S.; Ochterski, J.; Petersson, G. A.; Ayala, P. Y.; Cui, Q.; Morokuma, K.; Malick, D. K.; Rabuck, A. D.; Raghavachari, K.; Foresman, J. B.; Cioslowski, J.; Ortiz, J. V.; Baboul, A. G.; Stefanov, B. B.; Liu, G.; Liashenko, A.; Piskorz, P.; Komaromi, I.; Gomperts, R.; Martin, R. L.; Fox, D. J.; Keith, T.; Al-Laham, M. A.; Peng, C. Y.; Nanayakkara, A.; Gonzalez, C.; Challacombe, M.; Gill, P. M. W.; Johnson, B. G.; Chen, W.; Wong, M. W.; Andres, J. L.; Head-Gordon, M.; Replogle, E. S.; Pople, J. A. *Gaussian 98* (Revision A.9); Gaussian, Inc.: Pittsburgh, PA, 1998.

(35) Hobza, P.; Zaradník, R. *Intermolecular Complexes*; Elsevier: Amsterdam, 1988.

(36) van Duijneveldt-van de Rijdt, J. G. C. M.; van Duijneveldt, F. B.; van Lenthe, J. H. *Chem. Rev.* **1994**, *94*, 1873.

(37) Chalasinski, G.; Szczesniak, M. M. *Chem. Rev.* **1994**, *94*, 1723.

(38) Boys, S. F.; Bernardi, F. *Mol. Phys.* **1970**, *19*, 553.

(39) van Lenthe, J. H.; van Duijneveldt-van de Rijdt, J. G. C. M.; van Duijneveldt, F. B. *Adv. Chem. Phys.* **1987**, *124*, 521.

(40) Szalewicz, K.; Jeziorski, B. *J. Chem. Phys.* **1998**, *109*, 1198−1200.

(41) Mó, O.; Yáñez, M.; Elguero, J. *J. Chem. Phys.* **1997**, *107*, 3592.